Biomaterials 29 (2008) 3278–3288

Contents lists available at ScienceDirect

Biomaterials

journal homepage: www.elsevier.com/locate/biomaterials

An electrochemical fabrication process for the assembly of anisotropically oriented collagen bundles

Xingguo Cheng [a], Umut A. Gurkan [a], Christopher J. Dehen [b], Michael P. Tate [c], Hugh W. Hillhouse [c], Garth J. Simpson [b], Ozan Akkus [a,*]

[a] Weldon School of Biomedical Engineering, Purdue University, West Lafayette, IN 47907, USA
[b] Department of Chemistry, Purdue University, West Lafayette, IN 47907, USA
[c] School of Chemical Engineering, Purdue University, West Lafayette, IN 47907, USA

ARTICLE INFO

Article history:
Received 23 January 2008
Accepted 14 April 2008
Available online 9 May 2008

Keywords:
Assembly
Collagen
Electrochemistry
Biomimetic materials
Connective tissues

ABSTRACT

Controlled assembly of collagen molecules *in vitro* remains a major challenge for fabricating the next generation of engineered tissues. Here we present a novel electrochemical alignment technique to control the assembly of type-I collagen molecules into highly oriented and densely packed elongated bundles at the macroscale. The process involves application of electric currents to collagen solutions which in turn generate a pH gradient. Through an isoelectric focusing process, the molecules migrate and congregate within a plane. It was possible to fabricate collagen bundles with 50–400 μm diameter and several inches length via this process. The current study assessed the orientational order, and the presence of fibrillar assembly in such electrochemically oriented constructs by polarized optical microscopy, small angle X-ray scattering, second harmonic generation, and electron microscopy. The mechanical strength of the aligned crosslinked collagen bundles was 30-fold greater than its randomly oriented-crosslinked counterpart. Aligned crosslinked collagen bundles had about half the strength of the native tendon. Tendon-derived fibroblast cells were able to migrate and populate multiple macroscopic bundles at a rate of 0.5 mm/day. The anisotropic order within biocompatible collagenous constructs was conferred upon the nuclear morphology of cells as well. These results indicate that the electrochemically oriented collagen scaffolds carry baseline characteristics to be considered for tendon/ligament repair.

1. Introduction

As a natural protein, collagen is mainly responsible for the mechanical and structural integrity of load-bearing extracellular matrices in all vertebrates and several invertebrates. Rod-like collagen molecules self-assemble in a crystal-like fashion with different packing patterns and the resulting structures are cross-linked (CX) to form mechanically robust tissues *in vivo* [1]. More importantly, as in tendon and ligaments, type-I collagen molecules are anisotropically oriented in a preferred direction along the dominant physiological loading pattern [2]. As a biomaterial, collagen has been a key ingredient in tissue engineering scaffolds, wound healing biomaterials, drug/gene delivery agents, and nerve guide substrates [3,4]. The application range of collagen would be greatly broadened if the assembly process could be better controlled to facilitate the synthesis of dense and oriented tissue-like constructs [5].

There have been several efforts to render synthetic collagen structures with some degree of orientational anisotropy. The alignment of molecules by flow, mechanical extrusion, microfluidic channels, or anisotropic chemical nanopatterns has limitations in attaining high packing density, elastic deformability, and the final size of the construct [6–11]. Also, orienting collagen molecules by magnetic fields require tesla-order superconducting magnets due to low diamagnetic constant of collagen [12]. Collagen structures with liquid crystalline order can be synthesized by slowly increasing the collagen solution concentration during a lengthy (weeks to months) dehydration process [13]. Oriented collagen nanofibers can also be achieved by the electrospinning process [14]. However, this process has some limitations in terms of its cost-effectiveness and it involves the use of toxic and corrosive solvents. Therefore, there is currently a need to find alternative means of forming highly oriented and densely packed macroscale collagenous constructs with preparation timescales in the order of minutes to hours.

One alternative approach for providing high orientational order and packing density involves manipulation of the electrochemical environment surrounding collagen molecules. Previous studies

* Corresponding author. Tel.: +1 765 496 7517; fax: +1 765 496 1992.
E-mail address: ozan@purdue.edu (O. Akkus).

0142-9612/$ – see front matter © 2008 Elsevier Ltd. All rights reserved.
doi:10.1016/j.biomaterials.2008.04.028

investigated whether small electrical currents applied directly to collagen solutions played a role in the fibrillogenesis of collagen *in vitro* from a physiological bioelectricity point of view [15–17]. These studies demonstrated the emergence of a birefringent band between two electrodes which are dipped in collagen solutions. Early literature made a limited attempt to characterize electrochemically synthesized collagen structures and it was reported that there was a general lack of orientational anisotropy and the D-banding pattern was absent [16,17]. Therefore, the degree of fibrillar orientation, mechanical properties and other physicochemical characteristics of collagen constructs produced as such are currently ambiguous. Accordingly, the electrochemical process has been abandoned since the last 40 years.

Earlier attempts assumed the voltage and the current as the key variables in the electrochemical process, whereas the potential effects of peripheral factors such as the dimension and configuration of electrochemical cell were not taken into account. The first aim of this study was to improve the electrochemical synthesis process to form highly oriented and mechanically robust collagenous bundles (ropes) by using parallel wire electrodes. The level of improvement in the structural organization and mechanical properties were characterized by scanning electron microscopy (SEM), transmission electron microscopy (TEM), two-dimensional (2D) small angle X-ray spectroscopy (SAXS), second harmonic generation (SHG) methods, and tensile tests. Our second aim was to assess the baseline feasibility of the electrochemically synthesized collagen bundles for tissue engineering of connective tissues. The second aim was achieved by assessing the migration and proliferation, morphology, and orientation of cells seeded on the material. Three-dimensional (3D) constructs were constructed by grouping multiple oriented bundles together and the ability of the cells to populate the material was monitored.

2. Materials and methods

2.1. Preparation of aligned collagen bundles

The overall process included the following basic stages: (1) subjecting dialyzed collagen solution to electrochemical process which results in the formation of aligned collagen bundle, (2) treatment of the bundle in phosphate buffered saline (PBS) at 37 °C to promote fibrillogenesis, and (3) crosslinking in genipin to provide the final strength.

Fully dialyzed collagen was used as the electrolyte for the electrochemical alignment process. Ten milliliters of type-I collagen (6 mg/mL 97% from bovine hide; INAMED Corporation, Santa Barbara, CA) was dialyzed ($MW_{cut\ off} = 3.5$ kDa) against ultrapure water at 5 °C for 72 h to remove salts. The dialyzed collagen had the characteristics of normal acidic soluble monomeric collagen and did not undergo fibrillogenesis before the onset of the electrochemical process which took place at room temperature (Fig. 1a). The dialyzed collagen underwent fibril formation only after the addition of 10× PBS and adjustment of the temperature to 37 °C at pH 7.4 (Fig. 1a). This indicates that the dialyzed collagen mainly existed in molecular form instead of fibrillar form at the onset of electric current application.

The electrochemical process was carried out in a custom-made two-electrode electrochemical cell (Fig. 1b). Two stainless steel electrode wires (0.254 mm diameter, 25 mm length; Sigmund Cohen Corporation, New York) were stripped of their insulating sheet along an inch-long segment and positioned parallel to each other with about 1 mm spacing on a glass slide. The gap between the electrodes was filled with the dialyzed collagen solution which was a transparent viscous fluid. The electrochemical cell was placed in a closed glass Petri dish lined with moist bench paper to maintain humidity at room temperature. Electrodes were connected to a DC voltage source and a 1 MΩ resistor in series (Fig. 1b). At a supply voltage of 6 V, the current through the collagen solution was measured to be 3.5 μA and 2.5 V DC. The orientation of the forming collagen band was monitored by a polarized optical microscope (Olympus BX51, Melville, NY, USA) with the application of first order wavelength gypsum plate. For a positive birefringent material such as collagen, molecules which are aligned along the slow axis of this plate appear blue while those molecules which are aligned perpendicular to the slow axis appear yellow [18]. After the confirmation of the congregation and alignment of molecules along a band by polarized imaging, the current was interrupted, PBS was added, and the sample was collected with a pair of tweezers. This freshly aligned collagen bundles were incubated in 10× PBS solution (pH 7.4, 37 °C) for 12 h prior to crosslinking. The average dimension of bundles varied in the range of 50–400 μm diameter and 3–7 cm length depending on the length of electrodes. These aligned collagen bundles were crosslinked in 15 ml of 0.625% genipin (Wako Pure Chemical, Osaka, Japan) in a sterile 1× PBS solution at 37 °C for 3 days [19].

Randomly oriented collagen networks were used as controls to compare with aligned collagen made by the above electrochemical method. Randomly oriented collagen was prepared by mixing the dialyzed monomeric collagen solution with 10× PBS, casting on a glass surface as a layer, and by gelling at 37 °C. Strips were cut from this layer after crosslinking with genipin using fresh surgical blades. Native tendon bundles were obtained at the origin of the biceps muscle of a canine that was euthanized under the approval of the Purdue Animal Care and Use Committee. The tendon fibers were bleached in 1% NaOCl solution for 90 s to expose the collagen phase by removing the non-collagenous matter [20].

2.2. Small angle X-ray scattering (SAXS)

SAXS patterns were collected using a three-pinhole SAXS camera (Molecular Metrology, Texas, USA) with a microfocus X-ray source, an Osmic MaxFlux confocal X-ray optic, and a 2D Fujifilm image plate detector at a camera length of 1647 mm. The detector was calibrated using a silver behenate powder standard ($q = 0.107623$ Å^{-1}). The main beam intensity was attenuated with a beam stop blocking all scattering below $q = 0.11$ nm^{-1}. Plots of the intensity versus the magnitude of the scattering vector (q) were produced from a radial line plot of the 2D SAXS data along the direction of the fiber axis. The 2D SAXS scattering data was processed to calculate the order parameter as described earlier [21]. The intensity $I(\phi)$ of the strongest arc versus the azimuthal angle ϕ was obtained for tendon and the aligned crosslinked collagen. The integrals in Eq. (1) were carried out numerically and the order parameter S was obtained using Eq. (2). For an isotropic material, $S = 0$, and for an ideal uniaxially oriented material, $S = 1$.

$$\langle \cos^2 \phi \rangle = \frac{\int_0^{\pi/2} I(\phi) \sin(\phi) \cos^2 \phi \, d\phi}{\int_0^{\pi/2} I(\phi) \sin(\phi) d\phi} \quad (1)$$

$$S = \frac{1}{2}\left(3\langle \cos^2 \phi \rangle - 1\right) \quad (2)$$

2.3. Second harmonic generation (SHG) analysis

SHG analysis was performed to quantify the degree of orientation by using the discrete retardance nonlinear optical ellipsometer described previously [22] on samples of random-CX collagen gel, aligned-CX collagen bundles, and native tendon bundles. The SHG intensities were measured using different combinations of vertically (V) and horizontally (H) linearly polarized light for the incident and detected beams, with the vertical axis corresponding to the longer axis of the bundles. Samples were air dried, placed between two glass slides, and measured in the transmission configuration (0° tilt) as described earlier [22]. The SHG intensity was measured 9 times for each of the three samples, with 64 laser pulses per data point, and normalized to HHH. Reported standard deviations are dominated by sample-to-sample variance.

2.4. Scanning electron microscopy (SEM) and transmission emission microscopy (TEM)

Collagen samples were prepared using a procedure similar to that developed by Raub et al. for SEM imaging of collagen gels [23]. Dried samples were mounted on holders and coated with Pt for 40 s prior to imaging (FEI NOVA nanoSEM, FEI Company, Hillsboro, OR) using through-the-lens and Everhart–Thornley detectors at a 5 kV accelerating voltage. For TEM analysis, collagen samples were macerated in a depression slide using a scalpel and forceps in ultrapure water. About 10 μl of the supernatant was put on a TEM grid and allowed to settle for 1 min. Samples were stained with 1% phosphotungstic acid and dried prior to imaging by TEM (FEI/Philips CM-100, FEI Company, Hillsboro, OR).

2.5. Mechanical testing

Random-CX collagen bundles, aligned-CX collagen bundles prepared by the current electrochemical process, bleached tendon-CX, and native tendon fibers ($N = 10$/group) were tested for their tensile mechanical properties under similar conditions. Prior to tensile tests, samples were washed with deionized water, serially dehydrated in EtOH/H_2O solutions, and air dried. Both ends of the dried bundles were fixed on plastic tabs using epoxy and rehydrated with a 1× PBS. The thicknesses of rehydrated samples were measured using a confocal microscope (Olympus FV1000) and the width was measured using a calibrated video-microscope at five different locations along the gage length of bundles. The area that is measured the closest to the failure location was utilized for stress calculations. Samples were mounted on fixtures of an electromagnetically controlled materials testing machine (Testresources 800L, Shakopee, MN) and loaded in tension to failure monotonically in displacement control (10 mm/min). Load was measured by a load cell (10 lb, Omega Inc., Stamford, CT) and load values were divided by the area of the sample to calculate stress. The extension was normalized with the original gage length to calculate the strain. Elastic modulus was obtained by a linear regression fit. The

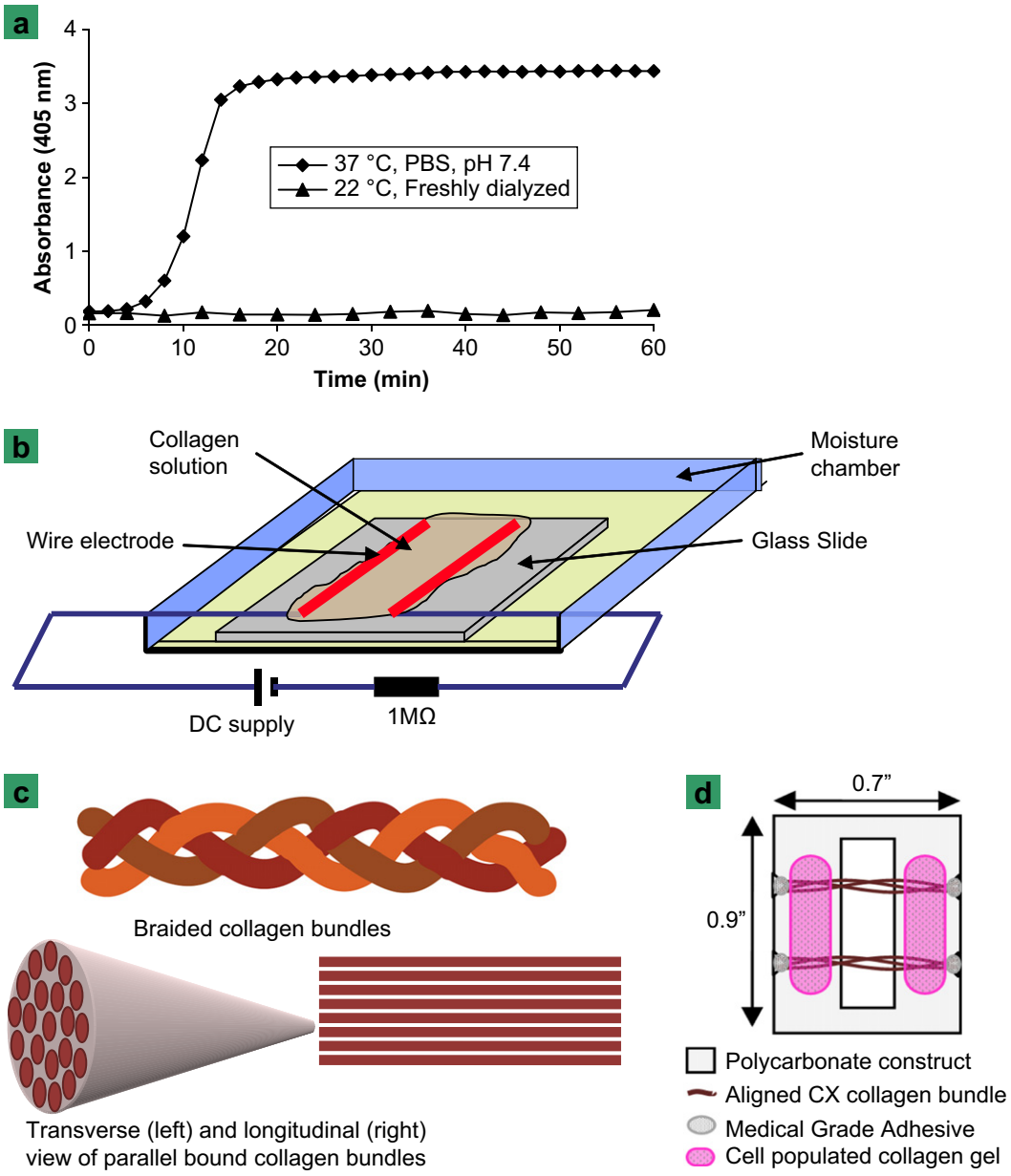

Fig. 1. (a) A dialyzed monomeric collagen is used as the stock for the electrochemical process. Turbidity test indicates that the stock solution does not form a gel at the room temperature. Gelation occurs only after the addition of PBS and adjusting the temperature to 37 °C. (b) Schema of the electrochemical cell used for the collagen assembly process. (c) Schematic representation of potential means by which 3D scaffolds can be constructed using individual bundles fabricated by the electrochemical process. Multiple bundles can be grouped together by braiding (top) or by parallel binding to form a synthetic collagen construct with desired dimensions. The bundles grouped together as such will have available inter-bundle space to allow cell migration and vasculogenesis. (d) Schema of the cell migration construct.

regression line extended between the end of the toe region and the midpoint of the linear elastic region.

2.6. Response of tendon-derived fibroblast cell cultures to the material

Achilles tendons of a 50-day old male Long-Evans rat (sacrificed under the approval of Purdue Animal Care and Use Committee) were harvested aseptically. Tendon specific fibroblasts were extracted and cultured by following established methods [24]. The cells demonstrated typical spindle-shaped fibroblast morphology and they were passed between three and five times before being used.

The collagen bundles themselves are densely packed and would not allow the migration of cells within, however, the envisioned practical use of these bundles for ligament/tendon replacement would involve grouping several bundles together (Fig. 1c). Cells would then migrate and populate the space between the bundles. So as to demonstrate the feasibility of this approach, a 3D bundle network was constructed by twisting three aligned-CX bundles together to form a 3D construct (approximately 0.5 mm diameter, 7 mm length). These dimensions correspond to the dimensions of a secondary fascicle in tendon's hierarchical organization.

The cell migration assay used in this study was modified from Cornwell et al. [25] and it utilized a migration template made out of polycarbonate (Fig. 1d). The collagen constructs were adhered to the template at the ends with medical grade adhesive (Loctite 4851), sterilized in 70% ethanol for 24 h, and air dried in the laminar flow hood before seeding.

The confluent rat-tendon derived fibroblasts were trypsinized, centrifuged, and the pellet was dispersed in a collagen gelation solution at a concentration of 30×10^5 cells/ml gel. The cell-containing collagen suspension was then poured on both sides of the migration template and incubated in CO_2-free incubator for 45 min for formation of collagen–cell lattice (Fig. 1d). Then growth media was added to submerge the collagen fibers and a portion of the collagen gel lattice. The construct was taken out after 7 days of incubation and examined for cell morphology and migration. The constructs were stained with Alexa Fluor 488 Phalloidin (Inivtrogen-Molecular Probes, Carlsbad, CA) and imaged under the fluorescent microscope. These cell-populated aligned CX collagen bundles were also fixed, embedded in paraffin, thin-sectioned, and stained by hematoxylin and eosin (H&E) stain.

2.7. Statistics

Significance of differences between groups was tested with a non-parametric one-way ANOVA (Kruskal Wallis), and if the difference was significant at $p < 0.05$, then differences between any two groups were further assessed by a

non-parametric Mann–Whitney U-Test with the level of significance set at $p < 0.05$ (Minitab, College Station, PA).

3. Results

3.1. Electrochemically induced collagen assembly process

The current density across the collagen solution (current density = current/height of collagen solution/length of electrodes) was about 0.55 A/m^2 and the nominal electric field strength ($E = V/d$, where V is the actual voltage across electrodes and d is the gap between electrodes) was about 2.5 kV/m. The electrochemical reactions in the solution are expected to be primary due to the electrolysis of water due to the following reasons: (a) the applied potential was greater than the electrolysis threshold (1.23 V) for water and (b) salts were removed from the solution by extensive dialysis.

$$\text{Anode}: \ 2H_2O - 4e^- \rightarrow 4H^+ + O_2; \ \text{cathode}: \ 4H_2O + 4e^- \rightarrow 4OH^- + 2H_2$$

These half-reactions resulted in the generation of a pH gradient between the electrodes, as confirmed by the color change after the addition of a universal pH-indicator dye (Fig. 2a). The solution near the anode became acidic, whereas the solution near the cathode became basic. This pH gradient had pronounced effects on the resulting assembly process. As the electrochemical process goes on, the randomly oriented collagen solution (magenta color) began to display interference colors in a region between the two electrodes (Fig. 2b). The emergence of a blue interference color indicated that aggregated collagen molecules were oriented parallel to the slow axis of the gypsum waveplate (i.e., oriented parallel to the long axis of the collagen band) [18]. Without the gypsum plate, the birefringence of the collagen solution composed of two components: molecules partially oriented as manifested by weak birefringence, and fully oriented collagen manifested by strong birefringence (Fig. 2c). The formation of the band took about 1 h at the applied current density of 0.55 A/m^2 and nominal electric field strength of 2.5 kV/m. Once the congregation and self-assembly of aligned collagen molecules were complete, it was observed that the pH of the assembled collagen band was around 9 (Fig. 2d, inset). The resulting collagen band assumed a densely packed and highly aligned conformation, as indicated by the strong birefringence (Fig. 2d). Band formation was observed in as short as 3 min at higher current densities and nominal electric field strength (e.g., voltage supply of 18 Volts with 1 MΩ resistor in a similar set up). Currently, we can fabricate several inches long bundles with 50–400 μm diameter by adjusting the electrode length, gap, current density, and nominal electric field (Fig. 2e). An aligned-CX collagen bundle was split open along its longer axis to expose the core region. SEM imaging showed that collagen bundle was closely packed and its fabric was oriented parallel to the longer axis of the fiber uniformly across the entire thickness (Fig. 2f).

3.2. Collagen orientation, structure, and fiber assembly

The structure of the aligned collagenous bundles formed by the parallel linear electrodes was compared with natural tendon fibers by compensated polarized optical microscopy. Native tendon fibers, as harvested, showed no uniform interference colors, due to the masking of collagen by other non-collagenous proteins and proteoglycans (Fig. 3a,b). After bleaching, the blue and yellow interference colors from the collagen have emerged along with the presence of a microscale periodic banding, the so-called "crimp pattern" [26]. Despite the lack of a strong crimp pattern, electrochemically synthesized collagen bundles showed interference colors similar to the bleached tendon, indicating that the degree of orientation for the natural and synthetic collagen bundles was comparable.

The 2D SAXS patterns (Fig. 3c–g) showed the evolution of the D-banding as the electrochemically aligned collagen was subjected to subsequent PBS and genipin treatments. Freshly aligned collagen did not show the periodic arc pattern (Fig. 3c), indicating that there is a lack of D-banding despite that the molecules are oriented and aggregated at the isoelectric point. However, the periodic arc pattern began to appear after the aligned collagen bundle was treated in PBS (Fig. 3d). The periodic arc pattern became more pronounced after PBS-treated aligned collagen was crosslinked in genipin (Fig. 3e). The SAXS pattern of the aligned-CX collagen had similarities to the SAXS pattern of the natural tendon (Fig. 3e,f). There is a considerable long-range order along the fiber axis in both aligned-CX collagen samples and the natural tendon. Upon comparison, it was observed that the azimuthal angular breadth of the Bragg diffraction peaks in the aligned-CX collagen sample (Fig. 3e) were even smaller than those observed in the natural canine tendon (Fig. 3f). The sharp Bragg diffraction peaks observed along the fiber axis in the aligned-CX collagen sample confirmed a staggered axial packing of the collagen molecules. By comparison with the natural canine tendon, many peaks were observed at nearly the same q-value, shifted only slightly to smaller spacings (Fig. 3g). The positions of all the diffraction peaks observed from each sample could be explained by a single periodic spacing D, given by $D = n2\pi/q_{peak}$, where n is the order of the peak 1, 2, 3, etc. Twelve peaks were observed for the natural tendon sample and yield a periodic distance of 62.4 nm (Table 1). The 12 peaks observed were the $n = 2$–13 peaks. The $n = 1$ peak hits the beam stop and was at too small of an angle to be observed by the experimental apparatus. The positions of all the observed peaks for the dried aligned-CX collagen sample can be explained by a slightly smaller D of 61.2 nm, which is in the lower range of characteristic period banding (60–70 nm) found in type-I collagen material [27–30]. Peaks corresponding to $n = 3$–13 were observed for aligned-CX collagen bundles. Both for tendon and the electrochemically synthesized collagen the $n = 6$ and $n = 9$ were the most intense peaks, further indicating that axial staggering of collagen molecules in the natural tendon and the aligned-CX sample is comparable. The calculations from the 2D SAXS scattering data indicated that the aligned crosslinked collagen had an order parameter of $S = 0.84$, whereas the natural tendon had $S = 0.69$ ($S = 1$ indicates perfect order, $S = 0$ indicates random isotropic structure).

The SHG analysis of the native tendon and the random-CX collagen samples served as reference points for assessing the order in the aligned-CX collagen constructs. In the absence of significant long-range in-plane order, one would expect relatively weaker SHG arising only from regions of local orientation in random collagen gels. Consistent with these expectations, the SHG efficiencies for the random-CX collagen gels were independent of the orientation within the plane, yielding similar low values for crossed (VHH/HVV) and coparallel (VVV/HHH) polarizations (Fig. 3h). The first index indicates the detected polarization state of the SHG photons and the last two indices indicate the polarization state of the two incident photons. The ratios obtained for the aligned-CX collagen construct suggested that these samples shared molecular-level structural similarities with the collagen in native tendon, and had significantly greater ($p < 0.0001$, $N = 27$) orientational uniformity than the random-CX collagen gel.

The lack of orientation in random collagen gels formed without the electrochemical process was confirmed by SEM imaging (Fig. 4a). Randomly oriented gels displayed the typical

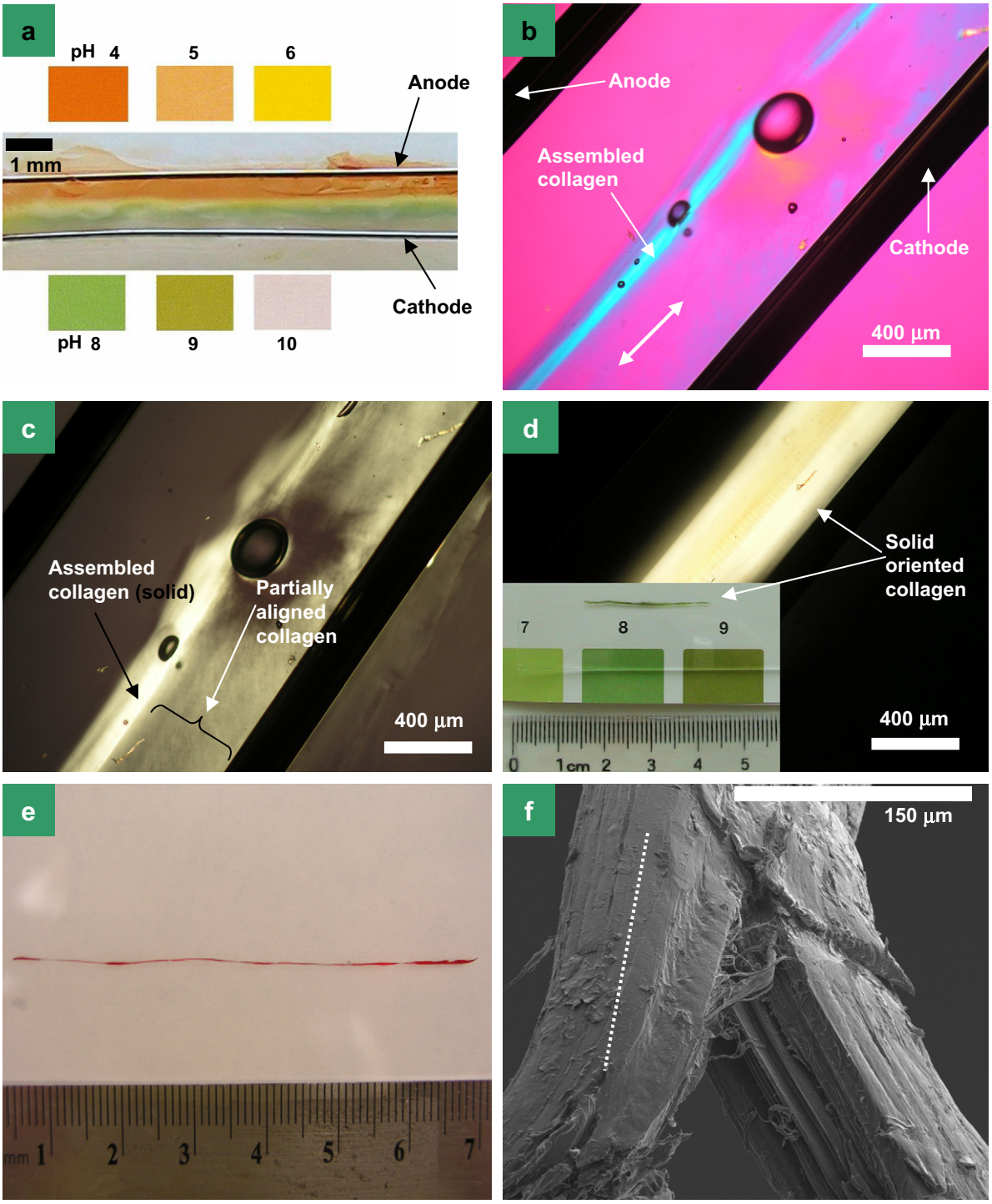

Fig. 2. The electrochemically induced collagen assembly process and the resulting product. (a) pH gradient in the collagen solution between electrodes as revealed by the universal pH-indicator dye. (b) Compensated polarized optical microscopic image showing that the collagen in the solution was congregated and assembled along a fixed band via isoelectric focusing. The blue color indicates that molecules are oriented parallel to the slow axis (double arrow) of the gypsum plate which is set parallel to electrodes. Bubbles were intentionally introduced by stirring to demonstrate that bubbles turn elliptical under the effect of convective forces. (c) Polarized optical image of 'b' which demonstrates that the rotary alignment of collagen molecules is ongoing in the region bounded by the band and the cathode as indicated by a relatively weaker birefringence. (d) The resulting collagen band after 1 h was in the solid phase and it was highly birefringent. The inset shows that the pH of the stained collagen bundle was in the vicinity of 9 (p*I* of collagen). (e) Image of a Sirius red stained individual aligned collagen bundle showing the dimensions (about 7 cm length and 400 μm diameter). (f) SEM image of a recovered aligned and crosslinked collagen bundle which was split along its longer axis (indicated by the broken line) intentionally to reveal the degree of packing and the uniformity of orientation along the longer axis of the bundle at the core region.

D-banding period around 63 nm as per TEM imaging (Fig. 4b). On the other hand, electrochemically aligned collagen bundles were composed of densely packed and uniformly oriented small fibers as evident by SEM imaging (Fig. 4c). For freshly aligned collagen sample, the TEM image shows the presence of aggregated fibrillar structures without any evidence of D-banding period (Fig. 4d). For aligned-CX collagen sample, TEM image was unsuccessful due to very dense packing, however, the presence of D-banding period in aligned-CX samples was confirmed by SAXS.

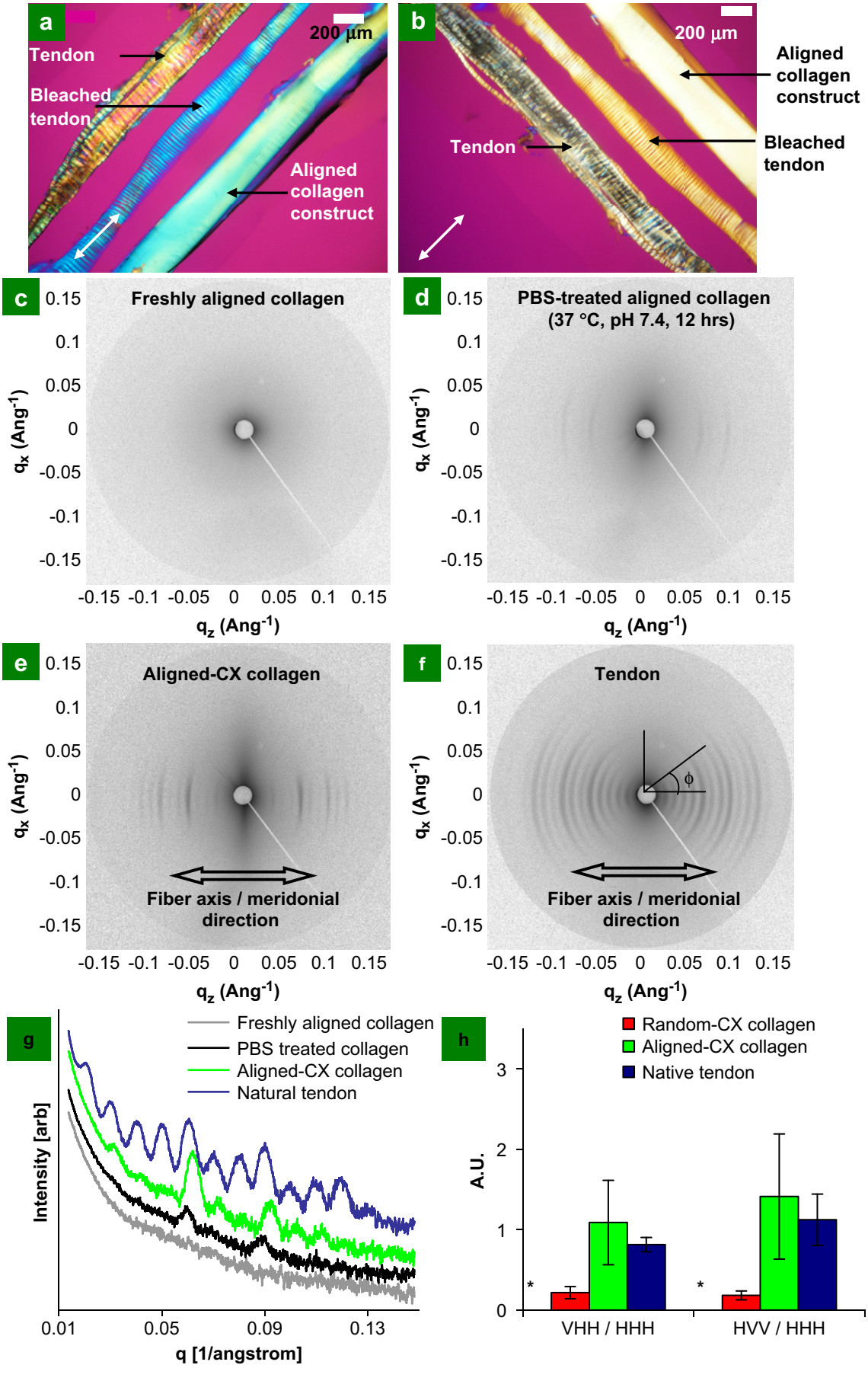
a
200 μm
Tendon
Bleached tendon
Aligned collagen construct
b
200 μm
Aligned collagen construct
Tendon
Bleached tendon
c
Freshly aligned collagen
d
PBS-treated aligned collagen (37 °C, pH 7.4, 12 hrs)
e
Aligned-CX collagen
Fiber axis / meridonial direction
f
Tendon
ϕ
Fiber axis / meridonial direction
0.15
0.1
0.05
0
-0.05
-0.1
-0.15
q_x (Ang^{-1})
q_z (Ang^{-1})
g
Freshly aligned collagen
PBS treated collagen
Aligned-CX collagen
Natural tendon
Intensity [arb]
0.01
0.05
0.09
0.13
q [1/angstrom]
h
Random-CX collagen
Aligned-CX collagen
Native tendon
A.U.
3
2
1
0
*
*
VHH / HHH
HVV / HHH

Table 1
Structural parameters obtained from the meridional reflections in the measured SAXS diffraction pattern

Order (n)	Native tendon		Aligned-CX collagen	
	q (1/nm)	d (nm)	q (1/nm)	d (nm)
1	–	62.4	–	61.2
2	0.2	31.2	–	–
3	0.3	20.8	0.32	19.9
4	0.4	15.6	0.4	15.7
5	0.5	12.5	0.52	12
6	0.61	10.4	0.62	10.1
7	0.7	8.91	0.72	8.7
8	0.8	7.8	0.83	7.6
9	0.9	6.93	0.93	6.8
10	1	6.24	1.02	6.1
11	1.1	5.67	1.13	5.6
12	1.2	5.2		
13	1.31	4.8		

From $D = n2\pi/q_{peak}$, it can be deduced that the D-banding of both collagenous materials are about 61–62 nm.

3.3. Mechanical properties of aligned-CX collagen bundles

Typical stress–strain curves for native tendon and aligned-CX collagen showed toe, heel, and linear regions (Fig. 5a) [31]. Aligned-CX collagen bundles had a 30-fold greater ultimate tensile strength and 25-fold greater tensile modulus than the random-CX collagen gel (Table 2, Fig. 5b,c, $p < 0.05$). The aligned-CX collagen bundles also had a 2-fold greater ultimate tensile strength and tensile modulus than the bleached-CX tendon (Fig. 5b,c, $p < 0.05$). The native tendon bundles were the strongest and stiffest of the five groups.

3.4. Fibroblast migration and proliferation on aligned-CX collagen bundles

Tendon-derived fibroblasts were able to migrate and proliferate within the 3D constructs formed by multiple bundles (Fig. 6a–c). The migration rate of fibroblast cells on 3D bundles was determined to be about 0.5 mm/day. H&E stained sections showed that the nuclei of fibroblasts on aligned-CX collagen bundles were elliptical, with their major-axis oriented along the bundles' longer axes (Fig. 6b, nuclear aspect ratio = major length/minor length = 2.3 ± 0.3), a morphology similar to those reported for tenocytes in native tendon fibers [32]. Histological images of braided bundle groups revealed that cells were able to migrate and infiltrate the space between bundles (Fig. 6c).

4. Discussion

This study has demonstrated that collagen can be assembled into highly oriented and densely packed rope-like long bundles by the electrochemical process described here. In this process, the major electrochemical reaction is mainly electrolysis of water since the electrochemical process is carried out in dialyzed collagen solution and no PBS (or other salts) was present. While we did not observe visible levels of corrosion, the dissolution of iron cations would be expected to occur from the 316 stainless steel electrode wires. So as to assess the level of interference from such ions, the electrochemical process was performed using inert Pt wire (A-Msystems, Washington, 125 μm diameter, 99.99% purity) electrodes and the outcome was similar to that reported for 316 stainless steel electrodes. However, when the resources allow, inert electrodes would be more suitable.

The migration and accumulation of collagen molecules along a defined band can be explained by the isoelectric focusing [33]. The existence of the pH gradient between electrodes causes differential charging of collagen molecules depending on their location. As an ampholytic molecule, the net charge of collagen molecules near the cathode become negative and the net charge of collagen molecules near the anode become positive [33,34]. Under the effect of the external electric field, charged collagen molecules migrate until they reach their isoelectric point, where they have no net charge. This results in the entrapment and assembly of collagen molecules at the p*I* plane, as viewed by the compensated polarized optical imaging (Fig. 2b). Isoelectric focusing has long been used for separation and congregation of ampholytic proteins in the general area of biotechnology and chromatography [33], however, the process has not been exploited as such for making biomimetic materials.

After the onset of the electrochemical process we observed the viscosity of the anode region to be visibly lower than the cathode region. There are several possibilities for this observed difference. First, the isoelectric point of collagen we used is around nine. In the anode region, pH is around four. In the cathodic region, the pH is around 11. So there is a steeper pH change from anode region ($\sim$5 units) to the p*I* line than from the cathode region to the p*I* line ($\sim$2 units). It is also possible that collagen molecules may be more charged in the anodic region compared to the cathodic region, resulting in greater repelling forces and faster migration of molecules from the anode side to the isoelectric plane. Second, according to the electrochemical reaction, the cathode side consumes water twice as much as the anode side. We observed that if the electrochemical cell was left active for over 24 h, the cathodic region would dry out while there would still be water in the anodic region. Third, basic pH at the cathodic side is known to promote collagen gelation [35], which may have increased viscosity. The validity of these possibilities requires further investigations.

While the migration of the collagen molecules can be reliably explained by isoelectric focusing, the mechanisms by which the rotational alignment of collagen molecules during the electrochemical process remain to be explained. Currently, we can speculate or, at best, propose a working hypothesis on this mechanism as follows. We believe that the electrostatic interactions between charged collagen molecules and the electric field play an important role. Charged functional groups are almost uniformly distributed along the length of the collagen molecule. As any ampholytic molecule, charges of functional groups are pH dependent [36]. Given the drastic pH change of the collagen solution from about 4 to 11 over 1 mm distance, we hypothesize that the change in hydrogen ion concentration over the length of one collagen molecule (300 nm) may be sufficient enough to vary the charge distribution along the molecule. Specifically, the end terminal of the molecule closer to the anode will be relatively more positively charged than the end terminal closer to the cathode, creating a pH induced electric dipole. Therefore, the end terminal closer to the anode will be electrostatically repelled more intensely by the anode than the end which is further away. The proposed

Fig. 3. Comparative analysis of the orientational anisotropy between tendon and the electrochemically aligned collagen bundle via compensated polarized optical microscopy, small angle X-ray scattering (SAXS), and second harmonic generation (SHG) analysis. (a) When the bundles were parallel to the direction of slow axis (white double headed arrow) of the gypsum plate in polarized optical microscope, both the bleached tendon and oriented collagen construct showed the blue retardation color. (b) When the bundles were rotated perpendicular to the slow axis of gypsum plate, both the bleached tendon and oriented collagen construct changed to the yellow retardation color. (c)–(f) SAXS patterns of the freshly aligned collagen, PBS-treated aligned collagen, aligned-CX collagen, and the natural tendon. (g) Intensity versus peak position of X-ray scattering. (h) SHG analysis of different groups of fibers. "*" denotes significant difference between random-CX group and the other two groups ($N = 27$, $p < 0.05$).

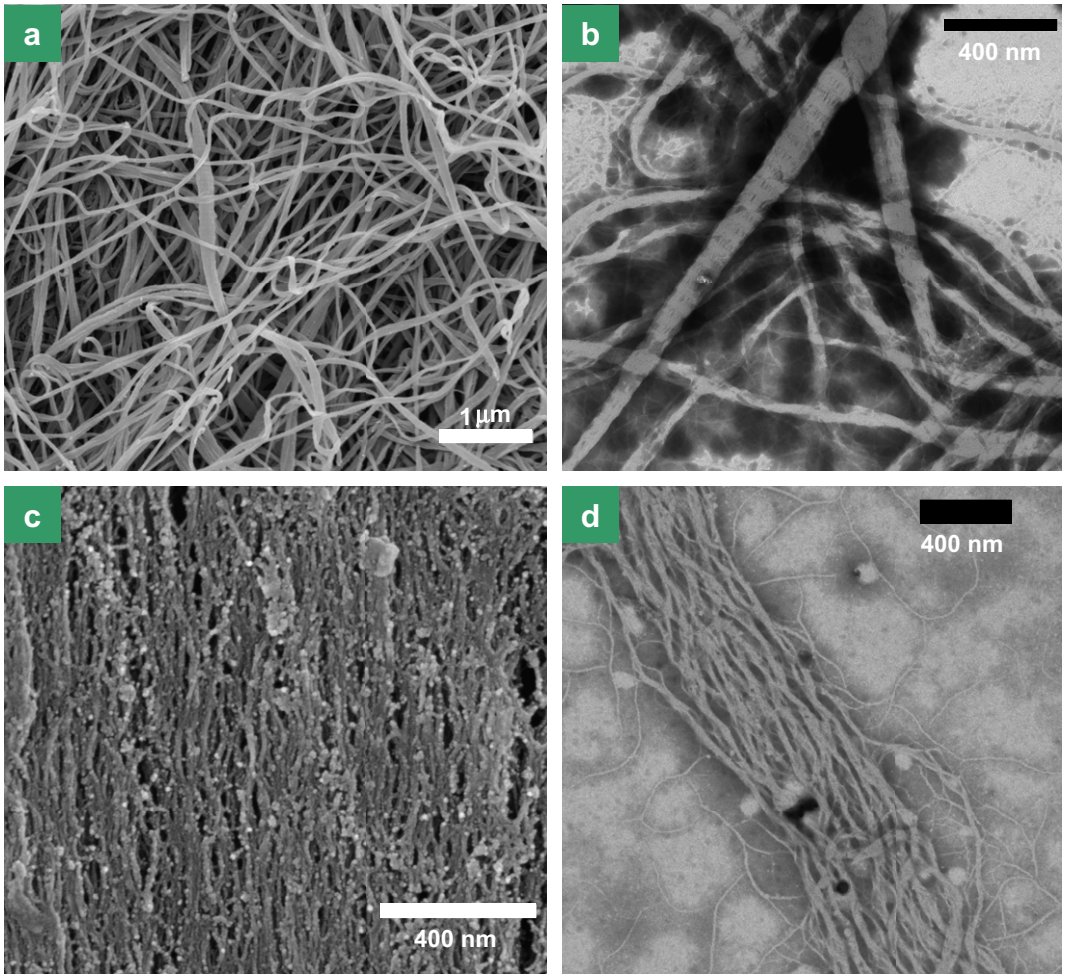

Fig. 4. (a) SEM image of a collagen gel prepared without employing the electrochemical process. The fabric displays a random network of big collagen fibers. (b) TEM image of the random collagen shows the D-banding in fibers. (c) SEM image shows that aligned collagen bundle prepared via the electrochemical method is composed of uniformly oriented small fibers. (d) TEM image of fibers teased from the freshly prepared aligned collagen bundle. Electrochemically synthesized fibers displayed fibrillar aggregates ranging from 5 to 40 nm diameter, which lacked the D-banding.

rotational electrostatic effect would gradually decrease as the molecule rotates to orient completely parallel to the electrodes. It is known that high electric field can induce the rotation of collagen molecule (Kerr effect) [37] and result in the birefringence of collagen solution. However, Kerr effect is due to the electrostatic interaction of intrinsic dipole of collagen molecules with high electric field during which molecules align parallel to the electric field. In the present case, molecules align perpendicular to the field. Therefore, the alignment mechanism of collagen in the current process appears to be different. Another possible alignment mechanism may be related to a physical phenomena. When aggregates of rods are compressed from both sides by the migration towards the p*I* plane, the rods may convectively cause each other to rotate. All of these potential mechanisms require electrostatic forces and charging of collagen molecules, both of which are controlled by nominal electric field strength and the pH gradient. So as to shed some light on the importance of electrostatic interactions and the pH gradient, we conducted an experiment with electrode separation distances of 1 mm, 2 mm, 7 mm, and 15 mm, while the actual voltage applied across the electrodes was maintained the same (2.5 V). The alignment of collagen diminished as the separation increased. It also took longer for the aligned band to appear at 7 mm than at 1 mm or 2 mm. At 15 mm separation, we did not observe the aligned collagen band to form within 24 h. At larger separation, the pH gradient is smaller, and, accordingly, the "electric dipole" acting upon each collagen monomer may become less pronounced. Also, the nominal electric field strength becomes smaller. These results suggest that electrostatic forces and a steep pH gradient are essential for rotational alignment of collagen monomers, yet the underlying mechanism remains to be elucidated.

An important detail to reproduce these results on different geometries/conformations would be the attainment of the current density and electric field strength as opposed to current and voltage. Current density accounts for the area over which the current flows and the field strength accounts for the separation between electrodes. Through a series of experiments, we observed the appropriate range for current density and electric field strength as 0.45–9.5 A/m^2 and 0.17–25 kV/m, respectively. The lower limits are associated with the formation of sufficient pH gradient via induction of electrolysis, whereas the higher limit of these ranges is determined by the bubble formation due to H_2 or O_2 release at the electrodes. The convection imposed by the formation of bubbles interferes with the alignment process.

Immediately after the electrochemical alignment, the collagen bundle had small fibrillar aggregates which lacked D-banding (Figs. 3c and 4d). The absence of D-banding at this stage of the process is expected due to several reasons. It is known that the electrostatic interactions between molecules are keys to staggering of neighboring molecules [38,39]. Since the alignment takes place

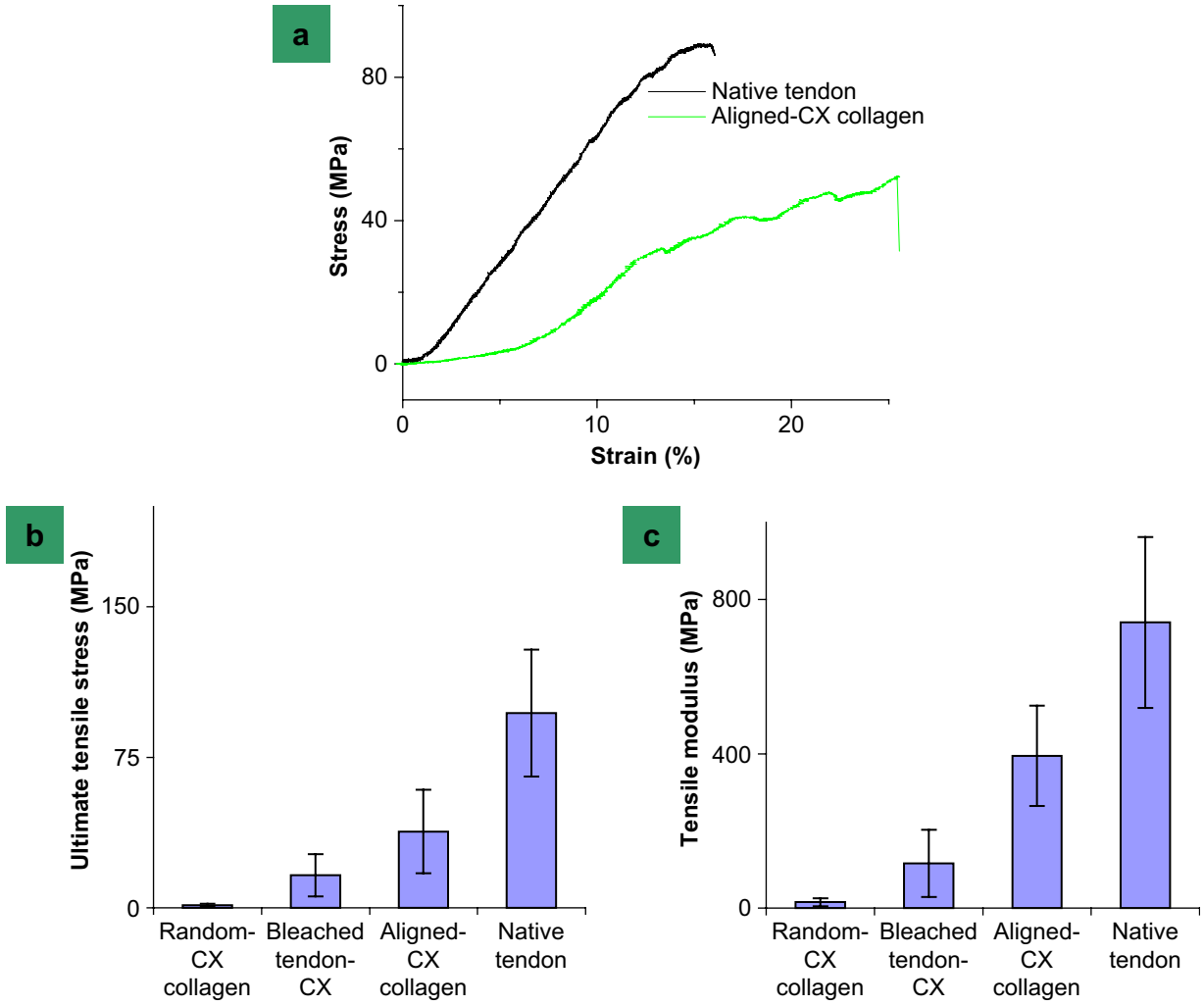

Fig. 5. (a) Typical stress–strain curves of aligned-CX collagen and native tendon. (b) Ultimate tensile stress and (c) tensile modulus ($N = 10$/group) of the groups involved in the study.

at the p*I*, the molecules lack charge; therefore, the formation of fibrils with D-banding would be unlikely. Furthermore, the solution was dialyzed free of salts, eliminating another essential ingredient for staggered fibril formation, sufficient ionic strength [40]. The D-banding emerged only after the incubation of the freshly aligned collagen at 37 °C in PBS buffered at pH 7.4. Therefore, the fibrillar aggregates formed following the electrochemical orientation are still in an energetically less favorable conformation and they can rearrange to assume D-banding under conducive conditions.

There are several unique advantages of the current electrochemical process: (1) environmentally friendly (no toxic solvents used compared to electrospinning to produce collagen fibers); (2) low cost (low electric voltage and current); (3) practicality of the experimental set up (pair of electrodes in a humid environment), which can be upgradeable to batch processing by employing electrode arrays; (4) ability to produce long rope-like constructs which may be useful in regeneration of longer tendons such as the flexors or extensors of the finger. It is possible to braid or group multiple bundles together to form larger macroscale dimensions. The most important advantage of the current electrochemical process is that it can produce highly oriented and closely packed collagenous constructs with mechanical properties converging upon those of natural tissues. The mechanical properties of aligned-CX collagen lie between those of native tendon and bleached-CX tendon fibers and are far higher than random-CX collagen gels. The packing density and the orientational order of fibrils clearly contributed substantially to the mechanical strength of the bundle. This observation also indicates that the degree of crosslinking and the presence of non-collagenous proteins and proteoglycans also contribute greatly to the strength and modulus of the tendon, in addition to the orientation factor. The mechanical properties of aligned collagen construct can be improved further by modifying electrochemical process variables and crosslinking conditions or via incorporation of other non-collagenous proteins and proteoglycans (e.g., decorin). Furthermore, this electrochemical alignment technique may potentially be applied to other fibrous proteins such as fibronectin, fibrinogen, or keratin.

Table 2
Tensile properties of collagen fiber bundles of different origin

	Random-CX collagen gel	Bleached tendon-CX	Aligned-CX collagen	Native tendon
Ultimate tensile stress (MPa)	0.8–2.5	6–30	24–88	57–148
Ultimate tensile strain (%)	6–17	11–25	7–24	10–20
Tensile modulus (MPa)	9–38	40–174	277–671	448–977

Reported values are the minimum and the maximum observations for a given parameter. All samples are crosslinked under similar conditions. $N = 10$ per/group.

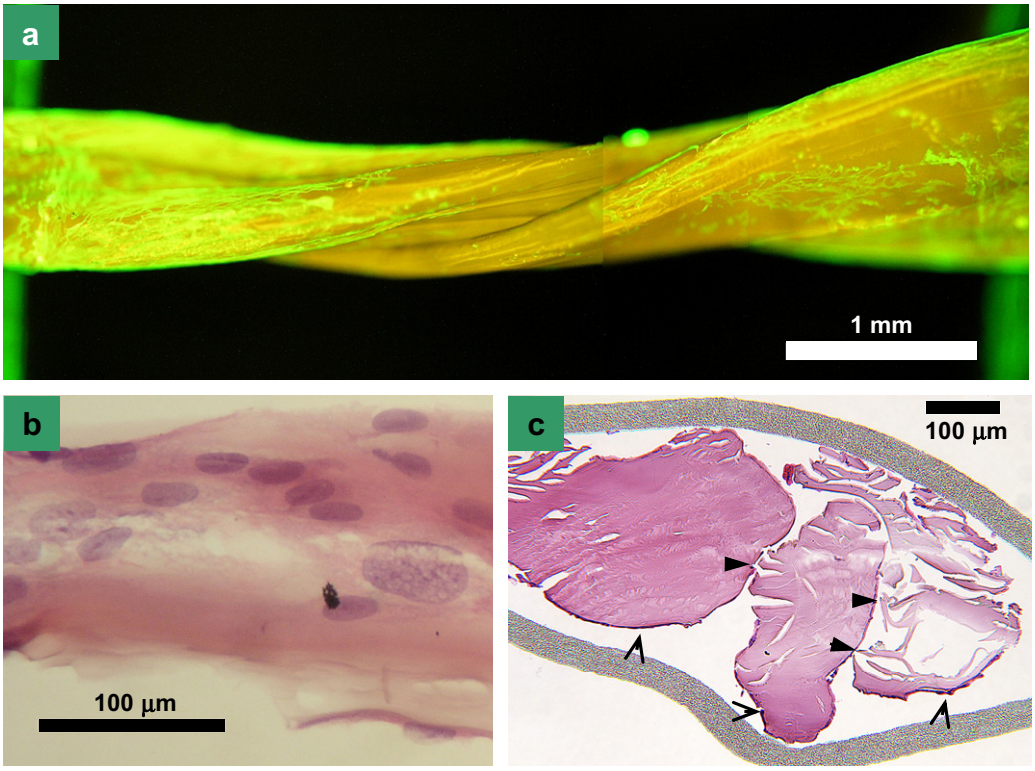

Fig. 6. (a) Tendon-derived fibroblast cells' migration and proliferation after 7 days on a construct prepared by twisting three collagen fiber bundles. (b) H&E stained histological sections taken along the longitudinal direction of bundles. Nuclei are stained in dark blue and they are elongated along the fabric orientation of the bundle. (c) Histological sections taken transversely to the longitudinal axis of a 3D construct composed of 3 bundles (sandwiched between two PTFE sheets to aid in histological processing). This micrograph confirms that the cells can migrate and populate the space in-between the bundles (►) as well as the outer surface of bundles (➢).

5. Conclusions

Highly oriented, densely packed, and mechanically robust collagen bundles have been successfully prepared by an electrochemical process. This process controlled the assembly of collagen molecules by combining the rotary alignment, isoelectric focusing, and assembly of collagen together. The cell migration assay indicated that the collagen material is conducive to cell proliferation and that it can impose its orientation on tendon cells. 3D bundle complexes also allowed cells to populate inter-bundle spaces. Therefore, this biomimetic material presents the baseline qualities to be considered for tendon/ligament repair.

Acknowledgements

This study was funded, in part, by various research grants from the National Science Foundation NSF CAREER-0449188 (O.A.), NSF-CHE 064059 (G.S.), and MRI program award 0321118-CTS (H.H) for *In-situ* X-ray Scattering from Nanomaterials and Catalysts. The authors would like to acknowledge Nicholas D. Wasserman for technical help with the mechanical tests, and Debby Sherman for excellent technical contributions to SEM and TEM imaging.

References

[1] Prockop DJ, Fertala A. The collagen fibril: the almost crystalline structure. Journal of Structural Biology 1998;122:111–8.
[2] Kato YP, Christiansen DL, Hahn RA, Shieh SJ, Goldstein JD, Silver FH. Mechanical-properties of collagen-fibers – a comparison of reconstituted and rat tail tendon fibers. Biomaterials 1989;10:38–41.
[3] Langer R, Vacanti JP. Tissue engineering. Science 1993;260:920–6.
[4] Lee CH, Singla A, Lee Y. Biomedical applications of collagen. International Journal of Pharmaceutics 2001;221:1–22.
[5] Sanchez C, Arribart H, Guille MMG. Biomimetism and bioinspiration as tools for the design of innovative materials and systems. Nature Materials 2005;4:277–88.
[6] Denis FA, Pallandre A, Nysten B, Jonas AM, Dupont-Gillain CC. Alignment and assembly of adsorbed collagen molecules induced by anisotropic chemical nanopatterns. Small 2005;1:984–91.
[7] Evans HJ, Sweet JK, Price RL, Yost M, Goodwin RL. Novel 3D culture system for study of cardiac myocyte development. American Journal of Physiology: Heart and Circulatory Physiology 2003;285:H570–8.
[8] Guo C, Kaufman LJ. Flow and magnetic field induced collagen alignment. Biomaterials 2007;28:1105–14.
[9] Lee P, Lin R, Moon J, Lee LP. Microfluidic alignment of collagen fibers for *in vitro* cell culture. Biomedical Microdevices 2006;8:35–41.
[10] Silver FH, Christiansen DL, Snowhill PB, Chen Y. Role of storage on changes in the mechanical properties of tendon and self-assembled collagen fibers. Connective Tissue Research 2000;41:155–64.
[11] Silver FH, Freeman JW, Seehra GP. Collagen self-assembly and the development of tendon mechanical properties. Journal of Biomechanics 2003;36:1529–53.
[12] Torbet J, Ronziere MC. Magnetic alignment of collagen during self-assembly. Biochemical Journal 1984;219:1057–9.
[13] Mosser G, Anglo A, Helary C, Bouligand Y, Giraud-Guille MM. Dense tissue-like collagen matrices formed in cell-free conditions. Matrix Biology 2006;25:3–13.
[14] Matthews JA, Wnek GE, Simpson DG, Bowlin GL. Electrospinning of collagen nanofibers. Biomacromolecules 2002;3:232–8.
[15] Becker RO, Bassett CAL, Bachman CH. Bioelectric factors controlling bone structure, Bone biodynamics. Boston: Little, Brown & Co; 1964.
[16] Eriksson C, Jones S. Effects of small electrical currents on collagen in solution. South African Journal of Science 1976;72:114–6.
[17] Marino AA, Becker RO. Effect of electric current on rat tail tendon collagen in solution. Calcified Tissue Research 1970;4:330–8.
[18] Martin R, Farjanel J, Eichenberger D, Colige A, Kessler E, Hulmes DJS, et al. Liquid crystalline ordering of procollagen as a determinant of three-dimensional extracellular matrix architecture. Journal of Molecular Biology 2000;301:11–7.
[19] Sung HW, Chang Y, Liang IL, Chang WH, Chen YC. Fixation of biological tissues with a naturally occurring crosslinking agent: fixation rate and effects of pH, temperature, and initial fixative concentration. Journal of Biomedical Materials Research 2000;52:77–87.
[20] Habelitz S, Balooch M, Marshall SJ, Balooch G, Marshall GW. *In situ* atomic force microscopy of partially demineralized human dentin collagen fibrils. Journal of Structural Biology 2002;138:227–36.

[21] Hillhouse HW, van Egmond JW, Tsapatsis M. Highly oriented mesostructured thin films: shear-induced deposition of optically anisotropic coatings of tungsten oxide surfactant composites. Langmuir 1999;15:4544–50.
[22] Dehen CJ, Everly RM, Plocinik RM, Hedderich HG, Simpson GJ. Discrete retardance second harmonic generation ellipsometry. Review of Scientific Instruments 2007;78:013106.
[23] Raub CB, Suresh V, Krasieva T, Lyubovitsky J, Mih JD, Putnam AJ, et al. Noninvasive assessment of collagen gel microstructure and mechanics using multiphoton microscopy. Biophysical Journal 2007;92:2212–22.
[24] Fini M, Torricelli P, Giavaresi G, Rotini R, Castagna A, Giardino R. *In vitro* study comparing two collageneous membranes in view of their clinical application for rotator cuff tendon regeneration. Journal of Orthopaedic Research 2007; 25:98–107.
[25] Cornwell KG, Lei P, Andreadis ST, Pins GD. Crosslinking of discrete self-assembled collagen threads: effects on mechanical strength and cell-matrix interactions. Journal of Biomedical Materials Research Part A 2007;80:362–71.
[26] Gathercole LJ, Keller A. Crimp morphology in the fiber-forming collagens. Matrix 1991;11:214–34.
[27] Baselt DR, Revel JP, Baldeschwieler JD. Subfibrillar structure of type-I collagen observed by atomic-force microscopy. Biophysical Journal 1993;65:2644–55.
[28] Belton JC, Michaeli D, Fudenberg HH. Freeze-etch study of collagen. 1. Native collagen from tendon and lung of rats. Arthritis and Rheumatism 1975;18: 443–50.
[29] Hosoyamada Y, Kurihara H, Sakai T. Ultrastructural localisation and size distribution of collagen fibrils in Glisson's sheath of rat liver: implications for mechanical environment and possible producing cells. Journal of Anatomy 2000;196:327–40.
[30] Yamamoto S, Hashizume H, Hitomi J, Shigeno M, Sawaguchi S, Abe H, et al. The subfibrillar arrangement of corneal and scleral collagen fibrils as revealed by scanning electron and atomic force microscopy. Archives of Histology and Cytology 2000;63:127–35.
[31] Fratzl P, Misof K, Zizak I, Rapp G, Amenitsch H, Bernstorff S. Fibrillar structure and mechanical properties of collagen. Journal of Structural Biology 1998;122: 119–22.
[32] Holmes I. Variations in tendon cell morphology with animal, site and age. Journal of Anatomy 1971;108:305–9.
[33] Garfin D, Ahuja S. Handbook of isoelectric focusing and proteomics. Elsevier academic press; 2005.
[34] Campbell MK, Farrell SO. Biochemistry. 5th ed. Brooks Cole; 2005.
[35] Hayashi T, Nagai Y. Effect of pH on stability of collagen molecule in solution. Journal of Biochemistry 1973;73:999–1006.
[36] Kadler K. Extracellular matrix-1-fibril-forming collagens – introduction. Protein Profile 1994;1:519–638.
[37] Kahn LD. Electric birefringence of macromolecular suspensions. Journal of Agricultural and Food Chemistry 1971;19:679–82.
[38] Gauba V, Hartgerink JD. Self-assembled heterotrimeric collagen triple helices directed through electrostatic interactions. Journal of the American Chemical Society 2007;129:2683–90.
[39] Freudenberg U, Behrens SH, Welzel PB, Muller M, Grimmer M, Salchert K, et al. Electrostatic interactions modulate the conformation of collagen I. Biophysical Journal 2007;92:2108–19.
[40] Williams BR, Gelman RA, Poppke DC, Piez KA. Collagen fibril formation – optimal *in vitro* conditions and preliminary kinetic results. Journal of Biological Chemistry 1978;253:6578–85.